RMetS
Royal Meteorological Society

Notes and Correspondence
Optimal control of katabatic flows within canopies

Hongbin Chen and Chuixiang Yi*
Queens College, City University of New York, Flushing, New York, USA

*Correspondence to: C. Yi, Queens College, CUNY, School of Earth and Environmental Sciences, 65-30 Kissena Blvd, Flushing, New York 11367, USA. E-mail: cyi@qc.cuny.edu

What slope angle favours the development of katabatic flow is still an open question. Some studies have clarified that katabatic winds are stronger on steep slopes, while others have demonstrated that katabatic winds are stronger on gentle slopes. Here, we explore the control mechanisms of katabatic flow using a simplified theoretical model in an attempt to clarify the causes of the paradoxical findings. Our results indicate that optimal conditions for katabatic flows within canopies are synergistically controlled by terrain angle, canopy structure and thermal condition through a simple equation $L_c V_T^{-2} \sin^3 \alpha = b$, where α is terrain slope, $L_c = 1/(c_D a)$ is canopy length-scale, c_D is drag coefficient, a is leaf area density, $V_T = R_c/\gamma$ is a thermal factor, R_c is a cooling rate, γ is ambient lapse rate, and b is a constant. This theoretical prediction implies that gentle slopes are optimal for katabatic flow developments in stably stratified air while steep slopes are optimal in weak or near-neutral stratification. Canopy effect is significant in the control of katabatic flows only on gentle slopes.

Key Words: katabatic flows; complex terrain; stratification; vegetation

Received 3 June 2011; Revised 14 January 2012; Accepted 20 January 2012; Published online in Wiley Online Library

Citation: Chen H, Yi C. 2012. Optimal control of katabatic flows within canopies. *Q. J. R. Meteorol. Soc.* DOI:10.1002/qj.1904

1. Introduction

Nearly 70% of Earth's land surface is covered with hills and mountains. Katabatic flows are a persistent feature over the rugged land surfaces. These flows participate in the redistribution of moisture, greenhouse gases and energy in the atmosphere. Consequently, they affect local weather (Hodur, 1997), including fog (Duynkerke, 1999), clouds (Bromwich *et al.*, 2001), rain (Steiner *et al.*, 2003) and snow (Massom *et al.*, 2001). In particular, the katabatic flows within a canopy (drainage flows) persistently exist even in cases where synoptic forcing is strong (Feigenwinter *et al.*, 2010a). These drainage flows result in many problems in measuring and modelling land–atmosphere interactions, such as serious advection errors in nocturnal eddy flux measurements (Goulden *et al.*, 1996; Massman and Lee, 2002; Aubinet *et al.*, 2003; Feigenwinter *et al.*, 2008, 2010a, 2010b; Finnigan, 2008; Foken, 2008; Kutsch *et al.*, 2008; Yi *et al.*, 2008; Montagnani *et al.*, 2009; Kochendorfer and Paw U, 2011). Therefore, studying the control mechanisms of katabatic flows within the canopy has many practical implications.

Physically, katabatic flows are associated with slope cooling, ambient stratification, slope angle, vegetation structure and other factors (Haiden and Whiteman, 2005; Yi *et al.*, 2005; Froelich and Schmid, 2006; Heinesch *et al.*, 2007, 2008; Sun *et al.*, 2007; Schaeffer *et al.*, 2008; Yi, 2009; Froelich *et al.*, 2011). This study explores the major controls of katabatic flows and how they work synergistically to produce maximum katabatic flows. These are still open questions even though katabatic flows have been studied for a long time since Prandtl (1952) first developed a one-dimensional model for katabatic flows. Particularly, there are two opposite findings of slope effects on katabatic flows. Some studies indicate that katabatic winds are stronger on steep slopes (Mahrt, 1982; Horst and Doran, 1986; Davies *et al.*, 1995; Princevac *et al.*, 2008), while others have demonstrated that katabatic winds are stronger on gentle slopes (Fleagle, 1950; Zhong and Whiteman, 2008; Axelsen and van Dop, 2009).

In this note, we attempt to clarify the theoretical causes of the above controversial findings based on a simplified model developed by Fleagle (1950), further modified by McNider (1982), and extended to include a vegetation layer by Yi (2009). Although the studies on katabatic flows mentioned above are all in the absence of a canopy, we prefer to use Yi's version of this kind of model with a forested slope since forested hills play an important role in ecosystem–atmosphere exchanges of materials and energy (Finnigan and Belcher, 2004).

2. Governing equations

Fleagle (1950) conceived of a simple layer model that treated a drainage layer equivalent to a parcel being cooled on a slope. McNider (1982), in a more formal development, then incorporated ambient stratification. In the McNider layer-model, he simply assumed that the model equations are valid for a drainage layer with idealized conditions that airflow is uniform along the slope except for a constant gradient of potential temperature consistent with the ambient stratification. Yi (2009) assumed that Fleagle–McNider's drainage parcel concept is valid within a canopy that has a uniform leaf area density (a) and drag coefficient (c_D), based on the data measured at Niwot Ridge AmeriFlux site (Fig. 8 in Yi *et al.*, 2005). The data indicate that wind speed and potential temperature were relatively uniform in a drainage layer within the canopy.

In mathematics, the governing equations of canopy flow are given by

$$\frac{\partial \bar{u}}{\partial t} = -g \sin\alpha \frac{\bar{\theta} - \theta_0}{\theta_0} - c_D a \bar{u}^2, \tag{1a}$$

$$\frac{\partial \bar{\theta}}{\partial t} = \gamma \bar{u} \sin\alpha - R_c \left(\frac{\bar{\theta} - \bar{\theta}_c}{\bar{\theta}_0 - \theta_c} \right), \tag{1b}$$

where $\bar{u}$ is the parcel velocity along the slope, $\bar{\theta}$ the parcel potential temperature, $\bar{\theta}_0$ the ambient potential temperature, θ_c potential temperature as the cooling rate is zero (Davis and McNider, 1997), g the gravitational acceleration, α the slope angle, γ ($= \partial\theta_0/\partial z$) the ambient lapse rate, R_c the parcel cooling rate. Although we attempt to include the vegetation effect on drainage flows, we want to clarify that this model is also valid for a bare slope. For a forested slope, the second term in Eq. (1a) represents a canopy drag ($F_d = -c_D a \bar{u}^2$), while for a bare slope, it represents a ground surface drag ($F_d = -k'' \bar{u}^2$). In both the models of Fleagle (1950) and McNider (1982), they assumed that the surface friction is proportional to wind speed, i.e. $F_d = -k\bar{u}$. In the present model, we prefer to use the velocity-squared law to represent land surface drag. Taylor was the first person to use $F_d = -k''\bar{u}^2$ to describe Earth's surface friction (Taylor, 1916). Since Taylor's investigation, $F_d = -k''\bar{u}^2$ has been tested and widely used (e.g. Sutcliffe, 1936; Deacon, 1949; Sutton, 1953). Therefore, our conclusion will be qualitatively valid in both cases, with and without canopy cover on the slope. Without the canopy, the $c_D a$ can be attributed to k'' that represents the property of a rough surface in causing surface drag for the fluid passing over it (Sutton, 1953).

3. Steady states and maximum flows

In this model, we pose a hypothesis that canopy thermal-slope flows are governed largely by buoyancy and drag forces. Physically, parcels initially cool and move downhill by gravity (Belcher *et al.*, 2008). At the beginning, drag force is smaller than the buoyancy force because wind speed is low and hence parcels are accelerated. Finally, a steady state is reached when these two forces are exactly balanced by increase of the drag force due to the acceleration and decrease of the buoyancy force due to warming from an adiabatic compression.

Mathematically, the steady states of katabatic flows can be determined by Eqs (1) through setting $\partial u/\partial t = 0$ and $\partial\theta/\partial t = 0$, i.e.

$$-\bar{u}_s^2 c_D a - \Delta\theta_s \frac{g \sin\alpha}{\theta_0} = 0, \tag{2a}$$

$$\bar{u}_s \gamma \sin\alpha - \Delta\theta_s \frac{R_c}{\theta_0 - \theta_c} - R_c = 0, \tag{2b}$$

where the subscript 's' indicates steady states, $\Delta\theta_s = \bar{\theta} - \theta_0$ is the potential temperature deficit. The steady solutions are as follows:

$$\bar{u}_s = \left(-1 + \sqrt{1 + \frac{4 c_D a R_c^2 \theta_0}{\gamma^2 g \sin^3\alpha (\theta_0 - \theta_c)}} \right) \frac{\gamma g \sin^2\alpha (\theta_0 - \theta_c)}{2 c_D a R_c \theta_0}, \tag{3}$$

$$\Delta\bar{\theta}_s = \left(-1 + \sqrt{1 + \frac{4 c_D a R_c^2 \theta_0}{\gamma^2 g \sin^3\alpha (\theta_0 - \theta_c)}} \right) \times \frac{\gamma^2 g \sin^3\alpha (\theta_0 - \theta_c)^2}{2 c_D a R_c^2 \theta_0} - (\theta_0 - \theta_c). \tag{4}$$

Here the negative solution of wind speed is discarded because we focus on katabatic flows.

For convenience in discussion, we write Eq. (3) in a more compact form

$$\bar{u}_s = (-1 + \sqrt{1 + \eta \sin^{-3}\alpha})\upsilon \sin^2\alpha, \tag{5a}$$

where

$$\eta = \frac{4 c_D a R_c^2 \theta_0}{\gamma^2 g (\theta_0 - \theta_c)}, \tag{5b}$$

$$\upsilon = \frac{\gamma g (\theta_0 - \theta_c)}{2 c_D a R_c \theta_0}. \tag{5c}$$

Katabatic flows attain a maximum speed at a certain value of $\sin\alpha$ as the other parameters are fixed, as shown in Figure 1. The conditions for maximum katabatic flows are required to satisfy the following equations:

$$\left.\frac{\partial \bar{u}_s}{\partial \sin\alpha}\right|_{\alpha_m} = \frac{\upsilon \sin\alpha_m}{2\sqrt{1 + \eta \sin^{-3}\alpha_m}} (\sqrt{1 + \eta \sin^{-3}\alpha_m} - 1) \times (\sqrt{1 + \eta \sin^{-3}\alpha_m} - 3) = 0, \tag{6a}$$

$$\left.\frac{\partial^2 \bar{u}_s}{\partial \sin\alpha^2}\right|_{\alpha_m} < 0. \tag{6b}$$

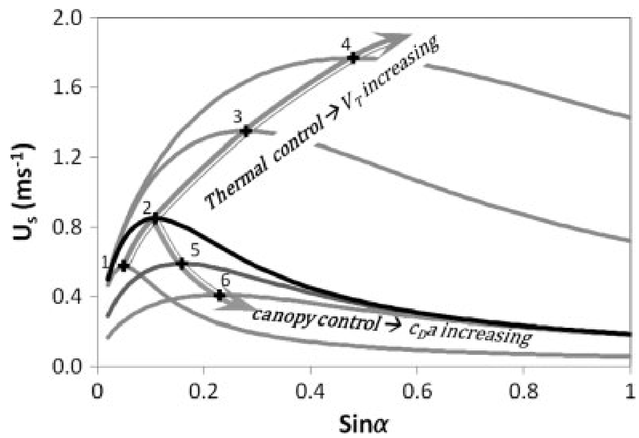

Figure 1. Illustration of katabatic wind speed versus the sine of the slope angle under different conditions of thermal control and canopy control. All six wind distributions are predicted by Eq. (5a). The black one is predicted with the values of the parameters: g = 9.8 m s^{-2}, γ = 2 K/km, $R_c = 3.74 \times 10^{-4}$ K/s, $(\theta_0 - \theta_c)/\theta_0 = 0.1$, $c_D = 0.15$ and $a = 0.5$ m^{-1}; the grey curves with the same values of the parameters except for different values of thermal factor ($V_T = R_c/\gamma$= 0.062, 0.748, 1.683 m s^{-1} for curves 1, 3 and 4, see Table 1) and the different values of canopy length-scale ($L_c = 1/(ac_D) = 4.4$, 1.5 m for curves 5 and 6, see Table 1). The grey double lines with arrows indicate how maximum katabatic wind speed shifts toward larger slope angles with increasing of the thermal factor and decreasing of canopy length-scale, respectively.

It is clear from the Eq. (6a) that

$$\frac{\partial \bar{u}_s}{\partial \sin\alpha} \begin{cases} \geq 0, & \text{when } \sin\alpha \leq \sqrt[3]{\eta/8} \\ < 0, & \text{when } \sin\alpha > \sqrt[3]{\eta/8} \end{cases} \tag{7}$$

Thus, the optimal conditions of katabatic flows are determined by a turning point (α_m) at which:

$$\sin\alpha_m = \sqrt[3]{\eta/8} = b^{\frac{1}{3}} V_T^{\frac{2}{3}} L_c^{-\frac{1}{3}}, \tag{8a}$$

or

$$L_c(V_T)^{-2}\sin^3\alpha_m = b, \tag{8b}$$

where $L_c = (cDa)^{-1}$ is a so-called canopy length-scale (Belcher *et al.*, 2003), $V_T = R_c/\gamma$ the thermal factor that is defined by the ratio of parcel cooling rate to ambient lapse rate, and $b = (2g)^{-1}\{\theta_0/(\theta_0 - \theta_c)\}$ taken as a constant with fixation of $\theta_0/(\theta_0 - \theta_c)$ at 10 following Davis and McNider (1997). Substituting Eq. (8a) into Eq. (5a), the maximum katabatic flows ($\bar{u}_{sm}$) can be expressed as a function of thermal factor and canopy length-scale:

$$\bar{u}_{sm} = g'(L_c V_T)^{\frac{1}{3}}, \tag{9}$$

where $g' = \sqrt[3]{0.25g(\theta_0 - \theta_c)/\theta_0}$.

According to Eq. (8a), the position ($\sin\alpha_m$) of maximum katabatic flows can be shifted from a small slope angle to a large slope angle by increasing the thermal factor (V_T) or decreasing the canopy length scale (L_c). For cases with a similar canopy length-scale (L_c = constant), a weak cooling rate or a strong stratification favours the occurrence of maximum katabatic flows on a gentle slope (see examples 1 and 2 of $\bar{u}_{sm}$ in Figure 1), while a stronger cooling rate or a weaker stratification favours the occurrence of maximum katabatic flows on a steep slope (the examples 3 and 4 of $\bar{u}_{sm}$ in Figure 1). For cases with a similar thermal condition (V_T = constant), although decreasing of canopy length-scale causes the position of the maximum katabatic flows to shift toward a larger slope angle (see examples 5 and 6 of $\bar{u}_{sm}$ in Figure 1), canopy control (L_c) on maximum katabatic flows is weaker than thermal control (V_T), in comparison with the examples 2, 5 and 6 with 1–4 of maximum katabatic flows shown in Figure 1 and listed in Table 1. Canopy effects on katabatic flows become diminished with increasing slope angles and can be ignored when the slope angle is greater than 30 degrees (Figure 1). Regardless of weather thermal control or canopy control, katabatic wind speed is more sensitive to slope angle on a smaller slope angle than on a large slope angle (Figure 1).

4. Concluding remarks

In this note we have derived the optimal conditions for the development of katabatic flows based on a simplified theoretical model. Katabatic flows are not governed by slope angle (gravity) alone, but controlled synergistically by slope cooling, ambient stratification and vegetation structure. The optimal condition Eq. (8b) with power-law elucidates that: (1) gravity plays the most important role in control of maximum katabatic flows due to the cubed $\sin\alpha$; (2) thermal control plays the second most important role due to the squared V_T^{-1}; and (3) canopy control plays less of a role than the gravity and thermal controls. The existence of maximum katabatic flow can be understood mainly as a result of competition between gravity and buoyancy. An increased slope causes the increasing of the gravitational acceleration on the drainage parcel. Meanwhile, the increased velocity means that the drainage parcel will be warmed by adiabatic compression heating through the first term on the r.h.s. of Eq. (1b). Consequently, the potential temperature deficit ($\Delta\theta = \bar{\theta} - \theta_0$) is reduced and hence the buoyancy term in Eq. (1a) becomes smaller. Thus, there is a point in the mid range of slope where maximum katabatic flow can be approached under conditions that all the other parameters, such as lapse rate, cooling rate, leaf area density and drag coefficient (or surface drag coefficient, k'', for the case without canopy) are fixed.

The condition of maximum katabatic flow production can be used to resolve the paradox that maximum katabatic flows can occur on either steep or gentle slopes. As illustrated in Figure 1, the location of maximum katabatic flows shifts from a small slope angle to a large slope angle with increasing thermal factor, $V_T = R_c/\gamma$. An increase in the thermal factor results from either increasing the cooling rate (R_c) or decreasing the lapse rate (γ). However, the thermal factor is more sensitive to variation of lapse rate than that of cooling rate because night-time cooling rate is proportional to $(273 + T)^4$ from the Stefan–Boltzmann law; here T is temperature in Celsius. To a good approximation by fixing the cooling rate, the values of the thermal factor are inversely proportional to lapse rate, and are lower with strong stratification and higher with weak stratification. Thus, Eq. (8) predicts that under strong stable stratification maximum katabatic flows occur on gentle slopes, while under weak stratification maximum katabatic flows occur on steep slopes. These theoretical predictions provide insights into why some studies reported the occurrence of strong katabatic flows on gentle slopes while others indicated the occurrence of maximum katabatic flows on steep slopes.

Table 1. Values of the maximum katabatic winds ($\bar{u}_{sm}$) shown in Figure 1 and associated parameters.

No.	$\bar{u}_{sm}$ (m s^{-1})	$\sin\alpha_m$	L_c (m)	V_T (m s^{-1})
1	0.59	0.053	13.3	0.062
2	0.85	0.110	13.3	0.187
3	1.35	0.278	13.3	0.748
4	1.77	0.477	13.3	1.683
5	0.59	0.159	4.4	0.187
6	0.41	0.229	1.5	0.187

It can be verified that all the ambient stratifications were stronger in the reported cases of occurrence of maximum katabatic flows on gentle slopes (e. g. Zhong and Whiteman, 2008; Axelsen and van Dop, 2009), and were weak in the reported cases of occurrence of maximum katabatic flows on steep slopes (e. g. Horst and Doran, 1986; Davies *et al.*, 1995; Princevac *et al.*, 2008).

The steady states of katabatic flows have been predicted by analytical models as: (1) an increasing function of slope angle, e.g. $\bar{u}_s \propto \sqrt{\sin\alpha}$ from Mahrt (1982), $\bar{u}_s \propto (\sin\alpha)^{2/9}$ from Nappo and Rao (1987); and (2) a decreasing function of slope angle, e.g. $\bar{u}_s \propto 1/\tan\alpha$ from Fleagle (1950), $\bar{u}_s \propto 1/\sqrt{\sin\alpha}$ from Axelsen and van Dop (2009). We expect that the increasing function of $\bar{u}_s$ with slope angle is valid under weak stratification conditions while the decreasing function of $\bar{u}_s$ with slope angle is valid under strong stratification conditions. These expectations are consistent with the results published in the literature excerpt in Mahrt's scale analysis (1982); here the relationship between his equilibrium solution and the ambient lapse rate was not clear. However, Mahrt pointed out that his equilibrium solution of katabatic flows is valid under high Froude number or low Richardson number. Therefore, Mahrt's solution is expected to be valid in weak stratification.

Our analysis indicates that in stably stratified air, gentle slopes are optimal for katabatic flow development, while in weak or near-neutral stratification, steep slopes are optimal. Canopy effect is significant in the control of katabatic flows only on gentle slopes. These conclusions are consistent with numerical simulation results (Xu and Yi, personal communication) and can serve as useful guidelines for future modelling and observational programmes.

Acknowledgements

This work was financially supported by the National Science Foundation under Grant No. 0930015. We are grateful for valuable comments and suggestions from two anonymous reviewers. We thank Xiyan Xu for her useful suggestions to improve our manuscript.

References

Aubinet M, Heinesch B, Yernaux M. 2003. Horizontal and vertical CO_2 advection in a sloping forest. *Boundary-Layer Meteorol.* **108**: 397–417.

Axelsen SL, van Dop H. 2009. Large-eddy simulation of katabatic winds. Part 2: Sensitivity study and comparison with analytical models. *Acta Geophys.* **57**: 837–856.

Belcher SE, Jerram N, Hunt JCR. 2003. Adjustment of a turbulent boundary layer to a canopy of roughness elements. *J. Fluid Mech.* **488**: 369–398.

Belcher SE, Finnigan JJ, Harman IN. 2008. Flows through forest canopies in complex terrain. *Ecol. Appl.* **18**: 1436–1453.

Bromwich DH, Cassano JJ, Klein T, Heinemann G, Hines KM, Steffen K, Box JE. 2001. Mesoscale modeling of katabatic winds over Greenland with the Polar MM5. *Mon. Weather Rev.* **129**: 2290–2309.

Davies TD, Palutikof JP, Guo X, Berkofsky L, Halliday J. 1995. Development and testing of a two-dimensional downslope wind model. *Boundary-Layer Meteorol.* **73**: 279–297.

Davis AMJ, McNider RT. 1997. The development of Antarctic katabatic winds and implications for the Coastal Ocean. *J. Atmos. Sci.* **54**: 1248–1261.

Deacon EL. 1949. Vertical diffusion in the lowest layers of the atmosphere. *Q. J. R. Meteorol. Soc.* **75**: 89–103.

Duynkerke PG. 1999. Turbulence, radiation and fog in Dutch stable boundary layers. *Boundary-Layer Meteorol.* **90**: 447–477.

Feigenwinter C, Bernhofer C, Eichelmann U, Heinesch B, Hertel M, Janous D, Kolle O, Lagergren F, Lindroth A, Minerbi S, Moderow U, Mölder M, Montagnani L, Queck R, Rebmann C, Vestin P, Yernaux M, Zeri M, Ziegler W, Aubinet M. 2008. Comparison of horizontal and vertical advective CO_2 fluxes at three forest sites. *Agric. Forest Meteorol.* **148**: 12–24.

Feigenwinter C, Montagnani L, Aubinet M. 2010a. Plot-scale vertical and horizontal transport of CO_2 modified by a persistent slope wind system in and above an alpine forest. *Agric. Forest Meteorol.* **150**: 665–673.

Feigenwinter C, Mölder M, Lindroth A, Aubinet M. 2010b. Spatiotemporal evolution of CO_2 concentration, temperature, and wind field during stable nights at the Norunda forest site. *Agric. Forest Meteorol.* **150**: 692–701.

Finnigan JJ. 2008. An introduction to flux measurements in difficult conditions. *Ecol. Appl.* **18**: 1340–1350.

Finnigan JJ, Belcher SE. 2004. Flow over a hill covered with a plant canopy. *Q. J. R. Meteorol. Soc.* **130**: 1–29.

Fleagle RG. 1950. A theory of air drainage. *J. Meteorol.* **7**: 227–232.

Foken T. 2008. The energy balance closure problem: An overview. *Ecol. Appl.* **18**: 1351–1367.

Froelich NJ, Schmid HP. 2006. Flow divergence and density flows above and below a deciduous forest. Part II. Below-canopy thermotopographic flows. *Agric. Forest Meteorol.* **138**: 29–43.

Froelich NJ, Grimmond CSB, Schmid HP. 2011. Nocturnal cooling below a forest canopy: Model and evaluation. *Agric. Forest Meteorol.* **151**: 957–968.

Goulden ML, Munger JW, Fan S-M, Daube BC, Wofsy SC. 1996. Measurements of carbon sequestration by long-term eddy covariance: Methods and a critical evaluation of accuracy. *Global Change Biol.* **2**: 169–182.

Haiden T, Whiteman CD. 2005. Katabatic flow mechanisms on a low-angle slope. *J. Appl. Meteorol.* **44**: 113–126.

Heinesch B, Yernaux Y, Aubinet M. 2007. Some methodological questions concerning advection measurements: A case study. *Boundary-Layer Meteorol.* **122**: 457–478.

Heinesch B, Yernaux Y, Aubinet M. 2008. Dependence of CO_2 advection patterns on wind direction on a gentle forested slope. *Biogeosciences* **5**: 657–668.

Hodur RM. 1997. The Naval Research Laboratory's Coupled Ocean/Atmosphere Mesoscale Prediction System (COAMPS). *Mon. Weather Rev.* **125**: 1414–1430.

Horst TW, Doran JC. 1986. Nocturnal drainage flow on simple slopes. *Boundary-Layer Meteorol.* **34**: 263–286.

Kochendorfer J, Paw U KT. 2011. Field estimates of scalar advection across a canopy edge. *Agric. Forest Meteorol.* **151**: 585–594.

Kutsch WL, Kolle O, Rebmann C, Knohl A, Ziegler W, Schulze E-D. 2008. Advection and resulting CO_2 exchange uncertainty in a tall forest in central Germany. *Ecol. Appl.* **18**: 1391–1405.

McNider RT. 1982. A note on velocity fluctuations in drainage flows. *J. Atmos. Sci.* **39**: 1658–1660.

Mahrt L. 1982. Momentum balance of gravity flows. *J. Atmos. Sci.* **39**: 2701–2711.

Massman WJ, Lee X. 2002. Eddy covariance flux corrections and uncertainties in long-term studies of carbon and energy exchanges. *Agric. Forest Meteorol.* **113**: 121–144.

Massom RA, Eicken H, Hass C, Jeffries MO, Drinkwater MR, Sturm M, Worby AP, Wu XR, Lytle VI, Ushio S, Morris K, Reid PA, Warren SG, Allison I. 2001. Snow on Antarctic sea ice. *Rev. Geophys.* **39**: 413–445.

Montagnani L, Manca G, Canepa E, Georgieva E, Acosta M, Feigenwinter C, Janous D, Kerschbaumer G, Lindroth A, Minach L, Minerbi S, Mölder M, Pavelka M, Seufert G, Zeri M, Ziegler W. 2009. A new mass conservation approach to the study of CO_2 advection in an alpine forest. *J. Geophys. Res.* **114**: D07306, DOI: 10.1029/2008JD010650.

Nappo CJ, Rao KS. 1987. A model study of pure katabatic flows. *Tellus* **39A**: 61–71.

Prandtl L. 1952. *Essentials of Fluid Dynamics*. Blackie and Son Ltd.

Princevac M, Hunt JCR, Fernando HJS. 2008. Quasi-steady katabatic winds on slopes in wide valleys: Hydraulic theory and observations. *J. Atmos. Sci.* **65**: 627–643.

Schaeffer SM, Anderson DE, Burns SP, Monson RK, Sun J, Bowling DR. 2008. Canopy structure and atmospheric flows in relation to the $\delta^{13}C$ of respired CO_2 in a subalpine coniferous forest. *Agric. Forest Meteorol.* **148**: 592–605.

Steiner M, Bousquet O, Houze Jr RA, Smull BF, Mancini M. 2003. Airflow within major Alpine river valleys under heavy rainfall. *Q. J. R. Meteorol. Soc.* **129**: 411–431.

Sun J, Burns SP, Delany AC, Oncley SP, Turnipseed AA, Stephens BB, Lenschow DH, LeMone MA, Monson RK, Anderson DE. 2007. CO_2 transport over complex terrain. *Agric. Forest Meteorol.* **145**: 1–21.

Sutcliffe RC. 1936. Surface resistance in atmospheric flow. *Q. J. R. Meteorol. Soc.* **62**: 3–14.

Sutton OG. 1953. *Micrometeorology: A study of physical processes in the lowest layers of the Earth's atmosphere*. McGraw-Hill.

Taylor GI. 1916. Skin friction of the wind on the Earth's surface. *Proc. R. Soc. London* **92**: 196–199.

Yi CX. 2009. Instability analysis of terrain-induced canopy flows. *J. Atmos. Sci.* **66**: 2134–2142.

Yi CX, Monson RK, Zhai ZQ, Anderson DE, Lamb B, Allwine G, Turnipseed AA, Burns SP. 2005. Modeling and measuring the nocturnal drainage flow in a high-elevation, subalpine forest with complex terrain. *J. Geophys. Res.* **110**: D22303, DOI: 10.1029/2005JD006282.

Yi CX, Anderson DE, Turnipseed AA, Burns SP, Sparks JP, Stannard DI, Monson RK. 2008. The contribution of advective fluxes to net ecosystem exchange in a high-elevation, subalpine forest. *Ecol. Appl.* **18**: 1379–1390.

Zhong SY, Whiteman CD. 2008. Downslope flows on a low-angle slope and their interactions with valley inversions. Part II: Numerical modeling. *J. Appl. Meteorol. Clim.* **47**: 2039–2057.

